11A.1 MOISTURE FLUX CONVERGENCE: ITS HISTORY AND APPLICATION IN CONVECTIVE INITIATION FORECASTING

Peter C. Banacos*
NOAA/NWS/NCEP/Storm Prediction Center
Norman, Oklahoma 73069

David M. Schultz
Cooperative Institute for Mesoscale Meteorological Studies, Univ. of Oklahoma, and
NOAA/National Severe Storms Laboratory, Norman, Oklahoma 73069

1. INTRODUCTION

Convective initiation (CI) remains a difficult forecast challenge (e.g., Ziegler and Rasmussen 1998; Moller 2001). Predicting the precise timing and location of deep moist convection, even along well-defined surface boundaries (e.g., fronts, drylines), remains a hurdle to improved short-range forecasts of severe weather and has been the subject of recent field work such as 2002's International H2O Project (IHOP) (Weckwerth et al. 2004).

In view of imperfect scientific knowledge concerning processes related to CI, as well as inadequacies in numerical guidance concerning, in particular, warm season convective storm evolution (Fritsch and Carbone 2004), forecasters have necessarily sought out a variety of diagnostic measures to aid in forecasting CI using derived parameters from both observations and numerical model output. One such diagnostic measure is moisture flux convergence (MFC). Reviews of the strengths and limitations of surface MFC have appeared in Doswell (1982), Bothwell (1988), and Waldstreicher (1989). This preprint provides some additional information; it traces the historical usage of MFC as a forecast tool to understand the physical rationale behind its origin, compares MFC to convergence through a scale analysis, and provides an example of elevated severe thunderstorm development (e.g. convective updrafts not rooted in the local boundary layer), a problem we feel deserves additional treatment of in the research community with the goal of improving forecast skill.

2. PHYSICAL EXPRESSION OF MFC

The expression for MFC arises from the conservation of water vapor in pressure (p) coordinates:

$$\frac{dq}{dt} = S\,, \tag{1}$$

where $$\frac{d}{dt} = \frac{\partial}{\partial t} + u\frac{\partial}{\partial x} + v\frac{\partial}{\partial y} + \omega\frac{\partial}{\partial p}\,,$$

$\mathbf{V}=(u,v,\omega)$, and q is the specific humidity. S represents the storage of water vapor, which is the difference between the sources and sinks of water vapor following an air parcel. S typically takes the form $E–C$, where E is the evaporation rate into the air parcel and C is the condensation rate into the air parcel. Many studies that employ (1) make the assumption that all the condensed water immediately precipitates out (P), so that $S=E–P$ (e.g., Palmén and Holopainen 1962). Using the continuity equation, $\partial u/\partial x + \partial v/\partial y + \partial \omega/\partial p = 0$, (1) can be expanded and rewritten in flux form, which conserves the total mass of moisture:

$$\frac{\partial q}{\partial t} + u\frac{\partial q}{\partial x} + v\frac{\partial q}{\partial y} + \omega\frac{\partial q}{\partial p} + q\left(\frac{\partial u}{\partial x} + \frac{\partial v}{\partial y} + \frac{\partial \omega}{\partial p}\right) = E - P \tag{2}$$

$$\underbrace{\frac{\partial q}{\partial t}}_{\substack{\text{local rate}\\ \text{of change}\\ \text{of } q}} + \underbrace{\nabla\cdot(q\mathbf{V}_h)}_{\substack{-\text{horizontal}\\ \text{MFC}}} + \underbrace{\frac{\partial}{\partial p}(q\omega)}_{\substack{-\text{vertical}\\ \text{MFC}}} = \underbrace{E-P}_{\substack{\text{sources}\\ \text{and sinks}}}\,, \tag{3}$$

where $\nabla = \hat{\mathbf{i}}\frac{\partial}{\partial x} + \hat{\mathbf{j}}\frac{\partial}{\partial y}$ and $\mathbf{V}_h=(u,v)$. Specifically (3) expresses the moisture budget for an air parcel, where the terms consist of the local rate of change of q, horizontal moisture flux divergence (the negative of horizontal MFC), the negative of vertical moisture flux convergence, and source and sink terms of moisture (specifically, evaporation and precipitation rates). By vector identity, horizontal MFC can be written as:

$$\text{MFC} = -\nabla\cdot(q\mathbf{V}_h) = -\mathbf{V}_h\cdot\nabla q - q\nabla\cdot\mathbf{V}_h\,, \tag{4}$$

$$\text{MFC} = \underbrace{-u\frac{\partial q}{\partial x} - v\frac{\partial q}{\partial y}}_{\substack{\text{advection}\\ \text{term}}} \underbrace{-q\left(\frac{\partial u}{\partial x} + \frac{\partial v}{\partial y}\right)}_{\substack{\text{convergence}\\ \text{term}}}\,. \tag{5}$$

In (5), the *advection term* represents the horizontal advection of specific humidity. The *convergence term* denotes the product of the specific humidity and horizontal mass convergence.

3. FORECAST UTILITY

The application of MFC in weather prediction has focused on three general topics: (1) calculation of large-scale precipitation fields within extratropical cyclones during the 1950s through mid 1960s, (2) as in integral

* Corresponding author address: Peter C. Banacos, Storm Prediction Center, 1313 Halley Circle, Norman, OK 73069; e-mail: peter.banacos@noaa.gov

component in the Kuo convective parameterization scheme developed in the 1960s, and, (3) severe local storm prediction beginning in 1970 as a direct result of (2). A more detailed treatment of the history of each of these areas is included in the following subsections.

3.1 Calculations of precipitation in midlatitude cyclones

Equation (3) can be solved for *P*–*E*, divided by the acceleration due to gravity *g*, and vertically integrated over the depth of the atmosphere from the surface $p=p_s$ to $p=0$ (Väisänen 1961; Palmén and Holopainen 1962), yielding

$$\overline{P}-\overline{E}=-\frac{1}{g}\int_0^{p_s}\frac{\partial q}{\partial t}dp-\frac{1}{g}\int_0^{p_s}\mathbf{V}_h\cdot\nabla q dp-\frac{1}{g}\int_0^{p_s}q\nabla\cdot\mathbf{V}_h dp\,, \quad (6)$$

where the overbar represents a vertical integrated quantity. If one assumes that evaporation $\overline{E}$ is small in areas of intense precipitation and saturation, and that local changes in water vapor content are primarily those owing to advection in synoptic-scale systems (such that the first two terms on the right-hand side are in balance, see references above), then

$$\overline{P}\approx-\frac{1}{g}\int_0^{p_s}q\nabla\cdot\mathbf{V}_h\,dp\,. \quad (7)$$

Thus, the precipitation amount is proportional to the vertically integrated product of specific humidity and mass convergence through the depth of the atmosphere.

The earliest synoptic application of (7) was from moisture budgets to estimate the large-scale precipitation in mid latitude cyclones using rawinsonde observations (Spar 1953; Bradbury 1957; Väisänen 1961; Palmén and Holopainen 1962; Fankhauser 1965). However, advances in numerical weather prediction almost certainly resulted in the phasing out of these attempts beginning in the 1960s, although the concept was theoretically sound (but also quite laborious). The case studies referenced above over the United States and the United Kingdom showed that precipitation calculated from (7) reproduced well the observed spatial pattern of precipitation and the maximum precipitation amount associated with mid latitude cyclones.

3.2 The Kuo Convective Parameterization Scheme

Kuo (1965, 1974) wished to quantify the latent heat release during condensation in tropical cumulonimbus, the main source of energy in tropical cyclones. He surmised that quantification of the water vapor budget might reveal the magnitude of the vertical motion and latent heat release indirectly. He derived the vertically integrated condensation minus evaporation $\overline{C}-\overline{E}$ as

$$\overline{C}-\overline{E}=(1-b)\,gM_t\,, \quad (8)$$

where *b* represents the storage of moisture and M_t is termed the *moisture accession*:

$$M_t=-\frac{1}{g}\left[\int_0^{p_s}\nabla\cdot(q\mathbf{V}_h)\,dp+F_{qs}\right]. \quad (9)$$

Moisture accession is the sum of a vertically integrated MFC and F_{qs}, the vertical molecular flux of water vapor from the surface. Kuo (1965) assumed that all the moisture accession goes into making clouds (i.e. $b=0$), a good assumption where tropical cumulus form in regions of deep conditional instability and large-scale surface convergence. Kuo (1974) found that *b* was much smaller than 1 in most situations and could be neglected in (9), leading to a direct relationship between the moisture accession and the condensation. Consequently, he argued that cumulus convection in the Tropics would be driven by the large-scale vertically integrated MFC.

It is important to note that the Kuo scheme was developed initially for tropical cyclone simulations, where the important question is "how much" latent heat will be released, not "will" latent heat be released. In contrast, the latter is often of central concern to convective forecasters in mid-latitudes, particularly in thermodynamic environments possessing an elevated mixed-layer (Carlson et al. 1983) and some degree of convective inhibition (CIN) through most (if not all) of the diurnal cycle. More formally, the Kuo formulation assumes convection processes moisture at the rate supplied by the environment (i.e. statistical equilibrium exists, Type I convection (Emanuel 1994)). Conversely, the sudden release of a finite, and typically large, amount of CAPE that has been built over time is a binary episode ("triggered" or Type II convection (Emanuel 1994)) in which the timing, and even the occurrence of the convection itself, remains a difficult and important forecast problem. This dilemma holds true for both forecasters and numerical simulations, as was alluded to in the introduction. These imperfections in applicability of MFC endured by forecasters help to explain "false-alarm" events in which well-defined axes of MFC exist but capping inversions preclude deep convective development in otherwise favorable environments.

3.3 Application of MFC to Mid Latitude Convection

Hudson (1970, 1971) was the first to compute vertically integrated MFC and to compare it to the amount of moisture required for cloud development in the midlatitudes for nine severe-weather events, interpreting the ratio between these two quantities as the fraction of convective cloud cover. He computed vertically integrated MFC over a depth from the surface to 10 000 ft (3048 m) MSL because "most of the water vapor is in this layer and because loss of wind data becomes significant above this level" (Hudson 1971, p. 759). Similarly, Kuo (1974) employed the top of his integration at 400 mb because of the perceived poor quality of the upper-air data above this level. Newman (1971), however, argued for using surface hourly observations to compute MFC because of their higher temporal and spatial resolution. As a result, he became the first to document the calculation of surface MFC.

The majority of studies since that time have computed surface, not vertically integrated, MFC, to take advantage of the better resolution. In Section 5 we conceptualize situations in which surface conditions may not be representative of data through a deeper layer, as well as non-surface based thunderstorm development, both of which limit the value of surface MFC in those specific scenarios.

Hudson (1970, 1971) and Newman (1971) found the best association between maxima of MFC and convective storms occurred 3 h *after* the time of the MFC analysis. This lag time suggested that surface MFC could be used as a short-range predictive parameter, and this has been noted in other MFC case studies (e.g., Doswell 1977; Negri and Vonder Haar 1980; Waldstreicher 1989). These investigations opened the door for usage of the parameter in real-time severe-weather forecast operations. In the early 1970s, implementation of surface MFC at the National Severe Storms Forecast Center (NSSFC, now the SPC) started with a computer program providing hourly printouts of gridded surface MFC plots 30 minutes after the hour (i.e., "data time"), which were then hand analyzed by duty forecasters[1] (Ostby 1975). Today, real-time hourly analyses of MFC and other severe weather parameters can be found from a wide variety of Internet sources, including the SPC mesoscale analysis page (http://www.spc.noaa.gov/exper/mesoanalysis/).

4. SCALE ANALYSIS

Recall from (5) that MFC can be written as the sum of two terms: the moisture-advection and convergence terms. In this section we explore what can be said about the behavior of these terms under synoptic and mesoscale conditions typically found with initiating deep moist convection.

4.1 Physical Considerations

We note that in mid latitude convective situations, the range of q falls generally between 5 and 30 g kg^{-1}; that is, q does not vary by more than one order of magnitude. On the other hand, horizontal divergence at the surface is highly scale dependent (Petterssen 1956), varying from 10^{-6} s^{-1} for synoptic- and planetary-scale flows to 10^{-3} s^{-1} near initiating surface-based thunderstorms (Ulanski and Garstang 1978). For synoptic-scale features with a time scale O(1 day) and a space scale O(1000 km), $|\mathbf{V}_h|$=O(10 m s^{-1}), q=O(10 g kg^{-1}), ∇q = O[1 g kg^{-1} (100 km)$^{-1}$], and $|\nabla \cdot \mathbf{V}_h|$=O($10^{-6}$ s^{-1}). Thus, the advection term $|\mathbf{V}_h \cdot \nabla q|$ is O(10^{-4} g kg^{-1} s^{-1}) and the convergence term $|q \nabla \cdot \mathbf{V}_h|$ is an order of magnitude smaller at O(10^{-5} g kg^{-1} s^{-1}). That the advection term dominates the convergence term is consistent with Rasmusson (1967), who found that advection of moisture is the dominant term in controlling the local change of moisture on the largest scales, including monthly and seasonal moisture budgets. The importance of Gulf of Mexico return flow northward across the Great Plains, in advance of spring upper troughs emerging from the southwestern U.S., is one well known example that emphasizes the importance of moisture advection on synoptic time scales prior to convective events.

On the scale of fronts, however, $|\nabla \cdot \mathbf{V}_h|$ is an order of magnitude larger, O(10^{-5} s^{-1}), such that both the advection and convergence terms are comparable at O(10^{-4} g kg^{-1}s^{-1}). For smaller mesoscale boundaries (e.g., lake/sea breezes, active or remnant convective outflow boundaries), or strong fronts, horizontal convergence $|\nabla \cdot \mathbf{V}_h|$ would be at least an order of magnitude larger, O(10^{-4} s^{-1}), implying dominance of the convergence term O(10^{-3} g kg^{-1} s^{-1}).

In a special observational network over south Florida (horizontal resolution of 2.5 km x 2.5 km and time resolution of 5 min), the magnitude of $|\nabla \cdot \mathbf{V}_h|$ was measured as high as 2.7x10^{-3} s^{-1} near developing convective updrafts (Ulanski and Garstang 1978). Observations of surface MFC of O(10^{-3} g kg^{-1}s^{-1}) are well documented in the vicinity of CI in severe-storm case studies (Ostby 1975; Negri and Vonder Harr 1980; Koch and McCarthy 1982). However, most standard wind observing networks are unable to resolve storm-scale convergence, which is likely O(10^{-2} g kg^{-1} s^{-1}) near robust updrafts. The spatial distribution of surface observations in vicinity of mesoscale boundaries and choices in objective analysis procedures can strongly influence the character of the MFC field as has been reported previously (e.g. Doswell 1977). Non-meteorological issues can negatively impact forecaster interpretation of the MFC field, and these problems have favored the complimentary use of remote sensing tools such as radar and visible satellite to better detect boundaries and low-level convergence in forecast practice.

4.2 Case Example

To compare directly the relative magnitude and spatial patterns of the convergence and advection terms, with both surface MFC and horizontal convergence, surface data for 1800 UTC 4 May 2003 are objectively analyzed at 40-km horizontal grid spacing (Fig. 1). This analysis is the operational objective-analysis routine employed by the SPC (Bothwell et al. 2002), which uses hourly RUC forecasts (Benjamin et al. 2004a, b) as the first-guess field. See Bothwell et al. (2002) for additional details about the technique.

At 1800 UTC 4 May 2003, a 990-mb low was centered near the northern Kansas and southern Nebraska border, with a warm front extending east-southeastward into western Missouri and a cold front extending west-southwestward along the surface wind shift in western Kansas and eastern Colorado (Fig. 1). Meanwhile, a dryline, extending southward from the low, was moving rapidly eastward across central Kansas, central Oklahoma, and north-central Texas, with a narrow surface moist axis (q ~ 16 g kg^{-1}) between the

[1] H. Hudson's move from NSSL in Norman, OK to the NSSFC in Kansas City, MO in 1971 likely aided in the implementation of MFC into the latter center's operational analysis routine.

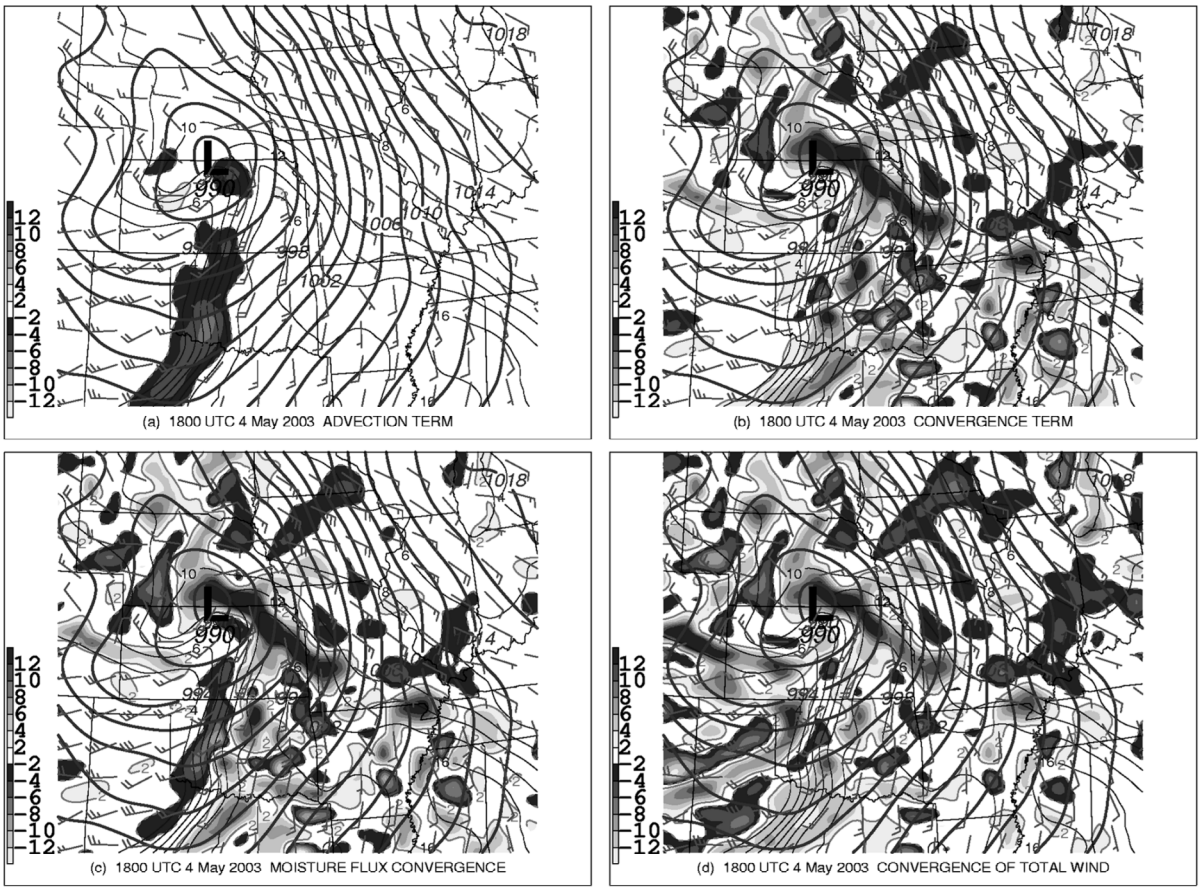

Fig. 1 Surface objective analysis valid at 1800 UTC on 4 May 2003. Sea-level pressure (thick solid lines every 2 mb), specific humidity (thin solid lines every 2 g kg^{-1}). Shaded regions represent (a) the moisture advection term in MFC expression (10^{-4} g kg^{-1} s^{-1}), (b) the convergence term in MFC expression (10^{-4} g kg^{-1} s^{-1}), (c) the total moisture flux convergence (10^{-4} g kg^{-1} s^{-1}), and (d) the convergence of the total wind (10^{-5}s^{-1}). Light-to-dark (dark-to-light) shadings represent positive (negative) values. Pennant, barb, and half-barb represent wind speeds of 25, 5, and 2.5 m s^{-1}, respectively.

dryline and warm front. An attendant strong 500-hPa short-wave trough was moving eastward from Colorado and New Mexico into the central plains states at this time (not shown). The upper-level forcing combined with low-level moisture and instability resulted in the development of isolated supercells beginning around 1815 UTC near the warm front in northeastern Kansas. Initiation of additional supercellular storms then occurred between 1900–2100 UTC, southward from the warm front along the convergence axis from southeastern Kansas into north-central Texas, just east of the dryline.

Negative moisture advection (–2 to –6x10^{-4} g kg^{-1} s^{-1}) is observed west of the progressive dryline, but positive areas of moisture advection of the same magnitude occur in only very small areas near the warm front in eastern Kansas and along the cold front in west-central Kansas (Fig. 1a). The convergence term (Fig. 1b) is most coherent near the surface low, along the warm front, and along the cold front in western Kansas and eastern Colorado. The convergence term is also large along the dryline (Fig. 1b). The convergence term is relatively effective in highlighting the boundaries of interest, with small-scale features (or noise from the RUC first guess) dominating elsewhere across the analysis domain. The surface MFC largely reflects the convergence term, with the exception of the strong negative area west of the dryline (cf. Figs. 1c and 1b).

The scaling arguments suggest that surface MFC can serve as an effective tool to detect mesoscale boundaries. However, surface convergence can serve the same purpose since it largely determines the surface MFC field. Forecasters may wish to compare MFC with convergence in convective situations to see these similarities.

5. CONCEPTUALIZED VARIATIONS OF CI

Through the continuity equation, storm-scale mass convergence is a necessary, but insufficient, condition for the development of thunderstorm updrafts. Unfortunately, the horizontal mass convergence associated with developing thunderstorms may not be well resolved. This may occur in one of two general situations; either the mechanism responsible for surface convergence is highly localized and not well sampled by observations, or the convergence is not located at or near the surface at all, but within the free atmosphere where observations are relatively sparse in time and space.

A conceptual diagram (see Fig. 2) illustrates commonly observed patterns of horizontal convergence as it relates to other ongoing processes in the atmosphere. In Fig. 2a, surface convergence is part of a deep tropospheric circulation as might be observed along a front with associated strong synoptic- or mesoscale forcing. These systems are efficient in eliminating convective inhibition through strong midlevel ascent, and the presence of moisture and instability often results in the surface horizontal mass convergence or MFC maxima being closely representative of the initiation location. Many published MFC case studies involve initiation of this type.

In Fig. 2b, the surface convergence is part of a shallow vertical circulation confined to the PBL, above which there is usually some convective inhibition. In the absence of large-scale forcing for ascent, or in the presence of midlevel subsidence, thunderstorm development may be precluded. When a capping inversion is not present, other factors may inhibit deep convective storms. For example, the magnitude of upward vertical motion may be insufficient to force parcels to their level of free convection. Alternatively, incipient updrafts may weaken because of entrainment of midlevel air with low relative humidity into the updraft. These factors are difficult to quantify in an operational setting and contribute in large measure to the uncertainty in short-range convective forecasts.

In Fig. 2c, the surface convergence is representative of a vertical circulation with considerable slope, such as along a warm front. In these situations, thunderstorm development may be horizontally displaced significantly from the convergence maxima and will be rooted above the local boundary layer (and above a relatively cool air mass). Such situations may help explain the observed displacement of storms downstream of the surface MFC maxima (e.g., Hirt 1982). Hail is the most common severe-weather threat from such elevated storms, with the potential for tornadoes and damaging winds reduced owing to the stable near-surface stratification. Other than the synoptic warm front as a candidate for such sloped ascent, operational experience suggests that subtle differences in boundary-layer characteristics arising from remnant outflow boundaries, differential cloud cover, or varying land surface characteristics can create localized regions of warm advection that can result in sufficient lift for thunderstorm development. The relative strength of convective inhibition (CIN) and

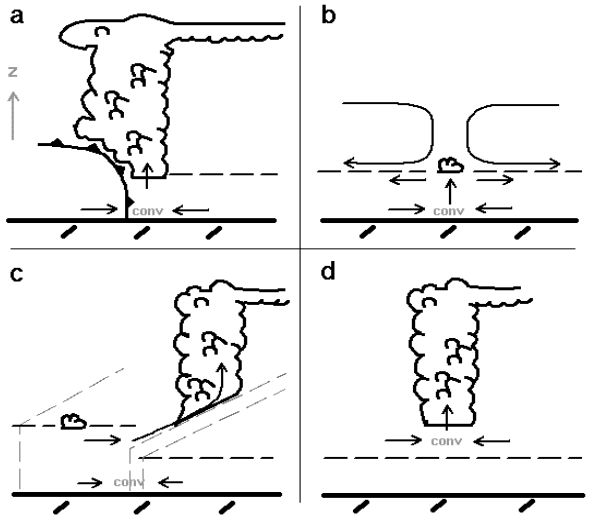

Fig. 2 Schematic of subcloud convergence (conv) as it relates to cumulus convection (represented by cloud outline). Arrows represent streamlines. Thick dashed line indicates top of PBL. (a) Convergence maximum is associated with a deep tropospheric circulation and deep moist convection. (b) Surface convergence maximum is associated with shallow cumulus development owing to midlevel subsidence and/or a capping inversion. (c) Surface convergence maximum is located near change in boundary layer height. Thin dashed line indicates isentropic surfaces in (c), with cooler surface air to the right. (d) Convergence maximum is rooted above the local boundary layer.

storm updrafts will then modulate the ability of the individual storms to become surface-based at some point after initiation. Elevated thunderstorms have been discussed by Colman (1990a, b) and Moore et al. (2003). We believe the forecast community could benefit from additional research in this area since sparse observations aloft often make elevated thunderstorm events difficult to forecast.

In Fig. 2d, subcloud convergence occurs above the PBL, such that an association between the surface horizontal mass convergence/MFC and CI does not exist. This situation is explored below.

5.1 An Elevated Thunderstorm Case

The surface objective analysis at 1500 UTC on 27 May 2004 shows a weak surface cyclone over southeastern Kansas, with a surface boundary and associated region of maximum convergence extending from northeastern Kansas eastward across northern sections of Missouri (Fig. 3d). This boundary was developed in part through outflow from early morning thunderstorms across eastern Kansas and central Missouri. Surface winds were generally southerly equatorward of the boundary, but became weak and ill-defined near and north of the surface convergence zone. Surface specific humidity values were about 12–13 g kg^{-1} over northern Missouri and southern Iowa. Consistent with the previous example in Fig. 1, the convergence term dominates the surface MFC (cf. Figs.

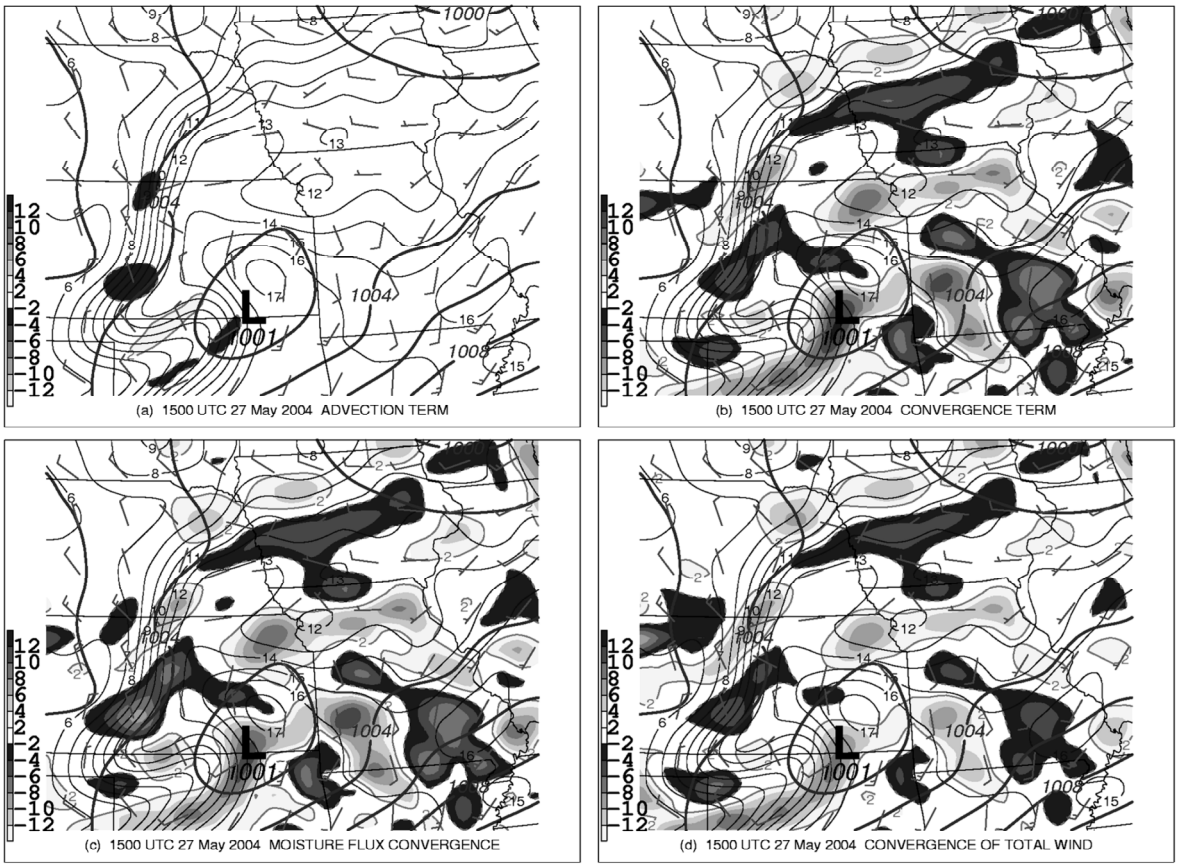

Fig. 3 As in Fig. 1, except for 1500 UTC on 27 May 2004, and specific humidity contour interval is 1 g kg^{-1}.

3b and 3c) because the advection term is relatively weak (Fig. 3a). Likewise, the similarity of surface MFC to surface horizontal mass convergence is quite striking (cf. Figs. 3c and 3d); surface MFC provides no tangible advantage to the forecaster over surface mass convergence in this case.

Visible satellite imagery reveals that the initial convective development occurred in southwest Iowa around 1515 UTC, displaced about 130 km north of both the surface MFC maxima (Fig. 4) and collocated surface boundary (Fig. 3d). The near-surface stable layer in 1200 UTC soundings at Topeka, Kansas, (Fig. 5a) and Omaha, Nebraska, (Fig. 5b) is likely inhibiting CI in the region of the surface boundary. An essential feature of the Topeka sounding pertinent to this case is the saturated layer at 820–780 mb (Fig. 5a). Parcels within this layer are potentially buoyant (CAPE ~ 1500 J kg^{-1}), though capped above by the elevated-mixed layer air around 700 mb. Additionally, the 780–530-mb layer is much warmer at Topeka than Omaha (cf. Figs 5a,b), with the temperature difference maximized near 700 mb (10°C at Topeka vs 4°C at Omaha). This strong gradient in mid-level temperature was located along and south of the upper-level cloud band evident in visible imagery from south-central Nebraska into central Iowa, which was associated with a compact short-wave trough across central Nebraska (not shown), likely aiding in synoptic-scale forcing for ascent.

A RUC initial proximity sounding at 1500 UTC in southern Iowa near the time of convective initiation is shown (Fig. 5c; location of sounding shown by "X" in Fig. 6). The sounding was modified slightly for 1500 UTC surface conditions near the developing storms using a temperature of 70°F (21.1°C) and a dewpoint of 62°F (16.7°C), yielding a surface-based convective inhibition of –80 J kg^{-1} (Fig. 5c). The RUC sounding does not resolve fully the moist layer between 800–750 mb. However, animations of visible satellite imagery indicate a distinct northward surge of moisture and a band of thicker stratus clouds (moving northward at around 10 m s^{-1}) into southwestern Iowa just prior to initiation, invigorating existing weaker convective updrafts in the region. Additionally, the 1455 UTC and 1515 UTC surface observations at Clarinda, Iowa (ICL), in east-central Page County (see Fig. 6 for the location), indicated broken clouds at 4900 ft (1493 m) AGL.

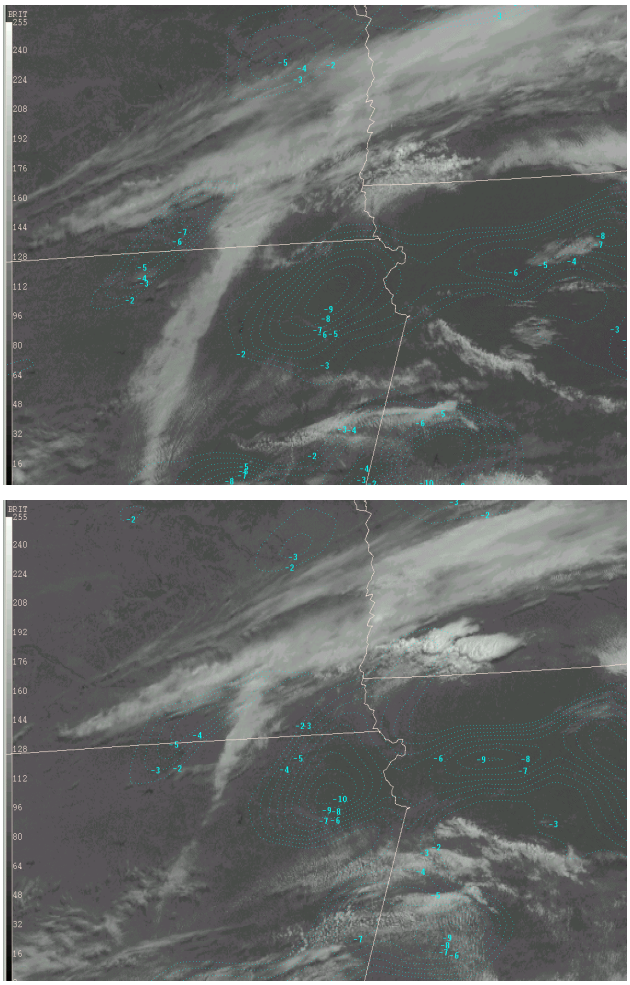

Fig. 4 GOES-12 1-km visible satellite imagery for 27 May 2004: (a, top) 1515 UTC and (b, bottom) 1602 UTC. Surface moisture flux convergence (dotted lines, 10^{-4} g kg^{-1} s^{-1}, negative values only) from SPC surface objective analysis (Bothwell et al. 2002) at (a) 1500 UTC and (b) 1600 UTC.

These observations were within 25 km of, and nearly coincident in time and space with, the initial development of deep moist convection. This cloud height corresponds well with the base height of the moist layer observed at Topeka at 1200 UTC. If the RUC sounding from southwest Iowa (Fig. 5c) is modified by the moist layer from the observed Topeka sounding (Fig. 5a), the sounding that results (Fig. 5d) yields a CAPE of 2100 J kg^{-1} without CIN for a parcel lifted from 820 mb. Combined with ascent provided by the approaching shortwave trough, this moist layer contributed to initiation of elevated supercells in prevailing strong westerly shear. The convection was quick to produce numerous reports of large hail and isolated damaging winds through 1900 UTC (Fig. 6). As the day progressed, diurnal heating reduced surface-based CIN and ultimately allowed thunderstorm updrafts to become rooted in the boundary layer and continue severe as they tracked southeastward across the northern half of Missouri with up to 4-in (10.2-cm) diameter hail and isolated tornadoes (not shown).

6. FINAL THOUGHTS

A forecaster's primary intent in the subjective use of surface MFC is to infer developing vertical circulations that might aid in the release of potential instability, allowing for CI. Application of surface MFC frequently works because convergence of the magnitude found along mesoscale boundaries implies dominance of the convergence term in the MFC equation; the modulating influence of q and moisture advection is comparatively small (except when extreme moisture advection exists, such as along a retreating dryline). The presence of sustained convergence infers upward vertical motion through continuity considerations.

We have highlighted a few caveats, which have been more or less described previously in a variety of contexts. First, a potentially unstable boundary layer air mass may be capped, and therefore the vertical circulation inferred from surface convergence is likely insufficient to carry air parcels to their LFC (e.g., Fig. 2b). Second, midlevel entrainment may curtail thunderstorm growth despite otherwise favorable conditions. Third, resolution of surface data may be inadequate to resolve the scale of surface horizontal convergence associated with the upward vertical motion. Fourth, the ascending branch of motion may contain considerable slope, allowing for "downstream" development of deep moist convection. Finally, the lower branch of a vertical circulation associated with deep moist convection may not occur at the surface, but aloft.

The version of the Eta model with the Kain–Fritsch cumulus parameterization (Kain et al. 2003b) provides as one of its outputs the pressure of the updraft source air (Kain et al. 2003a). Operational experience at the SPC with this field suggests that as much as 50% of thunderstorms have updraft source levels above the surface. Experience also suggests that the distinct nocturnal maximum in summertime convective rainfall over the Great Plains is often driven by elevated thunderstorm activity associated with the low-level jet (warm advection) or frontogenetic forcing.

More work from the research community, aimed at new predictive strategies for elevated thunderstorm development, would be beneficial to forecasters. Elevated CI underscores the importance of determining the source of moist and unstable air for thunderstorm development. Such situations curtail the more general applicability of surface diagnostics such as MFC, since near-surface conditions are not representative of convectively processed air. However, the frequency of correct forecasts can be increased through synthesis of available data resources in three-dimensions, including determination of potential source parcels and lift mechanisms for thunderstorms. Continued research on the convective initiation process under varying large-scale conditions and development of large sample compositing techniques promise to be fruitful approaches leading to the emergence of new

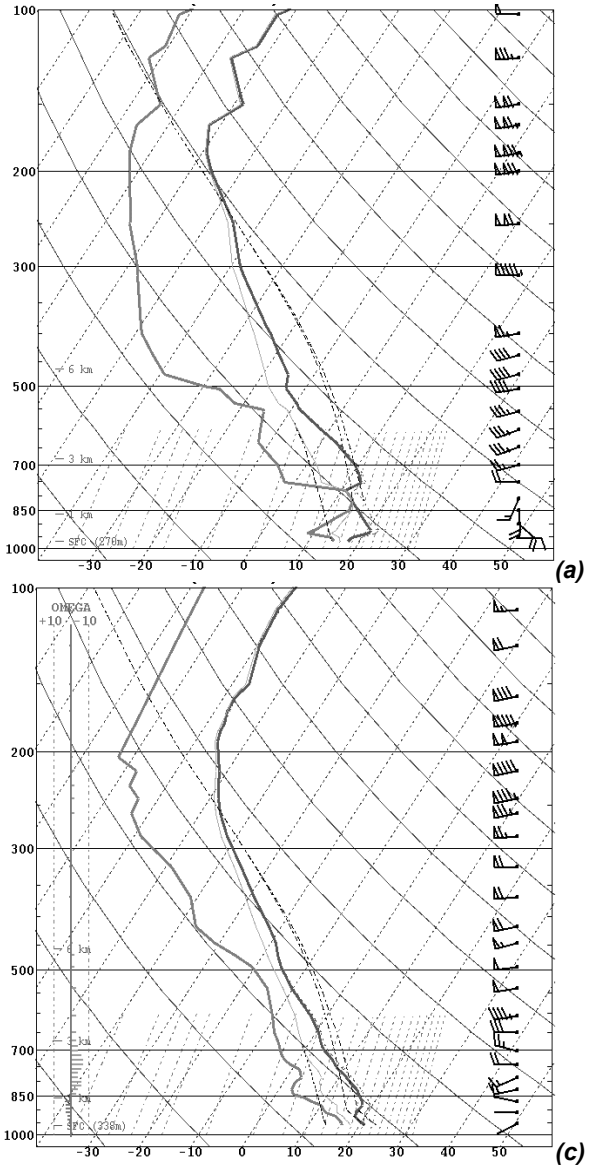

Fig. 5 Skew T–log p plots of observed temperature (dark gray lines) and dewpoint temperature (light gray lines) for 1200 UTC 27 May 2004: (a) Topeka, KS, and (b) Omaha, NE. (c) RUC-2 0-h forecast sounding with modified surface conditions valid 1500 UTC 27 May 2004 near the Missouri/Iowa border (see "X" in Fig. 6 for location). (d) As in (c), except sounding is modified using moist layer found on 1200 UTC Topeka sounding in (a). Horizontal bars represents vertical distribution of vertical motion (microbars s^{-1}). Pennant, barb, and half-barb represent wind speeds of 25, 5, and 2.5 m s^{-1}, respectively.

conceptual models, new forecast tools, and increased accuracy in CI forecasts in the years ahead.

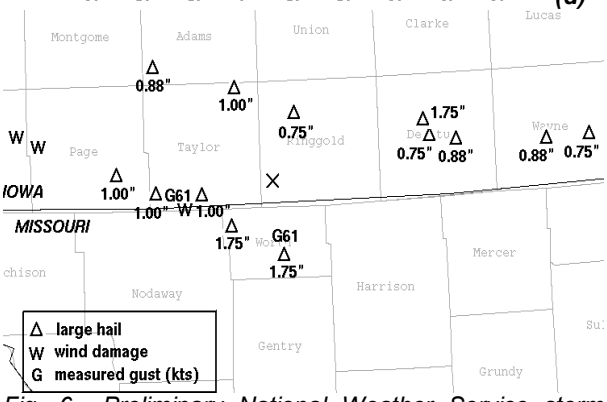

Fig. 6 Preliminary National Weather Service storm report data for 1600–1900 UTC 27 May 2004 across northern Missouri and southern Iowa. Location of RUC-2 sounding in Fig. 5 is denoted by "X" in southwestern Ringgold County, Iowa. County borders are indicated by the gray lines with county names listed within.

7. ACKNOWLEDGMENTS

We wish to thank the following individuals for their discussions pertaining to this research: Phillip Bothwell (SPC), Chuck Doswell (OU/CIMMS), Bob Johns (OU/CIMMS), Jack Kain (NSSL), Jim Moore (St. Louis Univ.), and Steve Weiss (SPC). Funding for Schultz was provided by NOAA/OAR/NSSL under NOAA–OU Cooperative Agreement NA17RJ1227.

REFERENCES

Benjamin, S. G., G. A. Grell, J. M. Brown, T. G. Smirnova, and R. Bleck, 2004a: Mesoscale weather prediction with the RUC hybrid isentropic-terrain-following coordinate model. *Mon. Wea. Rev.,* **132**, 473–494.

_____, S. G., D. Dévényi, S. S. Weygandt, K. J. Brundage, J. M. Brown, G. A. Grell, D. Kim, B. E. Schwartz, T. G. Smirnova, T. L. Smith, and G. S. Manikin, 2004b: An hourly assimilation-forecast cycle: The RUC. *Mon. Wea. Rev.,* **132**, 495–518.

Bothwell, P. D., 1988: Forecasting convection with the AFOS Data Analysis Programs (ADAP-VERSION 2.0), NOAA Technical Memorandum NWS SR-122, NOAA/NWS Southern Region, Fort Worth, TX, 92 pp.

_____, J. A. Hart, and R. L. Thompson, 2002: An integrated three-dimensional objective analysis scheme in use at the Storm Prediction Center. Preprints, *21st Conf. Severe Local Storms,* San Antonio, TX, Amer. Meteor. Soc., J117–J120.

Bradbury, D. L., 1957: Moisture analysis and water budget in three different types of storms. *J. Meteor.*, **14**, 559–565.

Carlson, T. N., S. G. Benjamin, G. S. Forbes, Y.-F. Li, 1983: Elevated mixed layers in the regional severe storm environment: conceptual model and case studies. *Mon. Wea. Rev.*, **111**, 1453-1474.

Colman, B. R., 1990a: Thunderstorms above frontal surfaces in environments without positive CAPE. Part I: A climatology. *Mon. Wea. Rev.,* **118,** 1103-1122.

_____, B. R., 1990b: Thunderstorms above frontal surfaces in environments without positive CAPE. Part II: Organization and instability mechanisms. *Mon. Wea. Rev.,* **118,** 1123–1144.

Doswell, C. A. III, 1977: Obtaining meteorologically significant surface divergence fields through the filtering property of objective analysis. *Mon. Wea. Rev.*, **105**, 885-892.

_____, 1982: The operational meteorology of Convective weather, Volume 1; Operational mesoanalysis, NOAA Technical Memorandum NWS NSSFC-5, NOAA/NWS National Severe Storms Forecast Center, Kansas City, MO.

Emanuel, K. A., 1994: *Atmospheric Convection*. Oxford University Press, New York, 580 pp.

Fankhauser, J. C., 1965: A comparison of kinematically computed precipitation with observed convective rainfall. National Severe Storms Laboratory Report 25, Norman, OK, 28 pp.

Fritsch, J. M., and R. E. Carbone, 2004: Improving quantitative precipitation forecasts in the warm season: a USWRP research and development strategy. *Bull. Amer. Meteor. Soc.*, **85**, 955-965.

Hirt, W. D., 1982: Short-term prediction of convective development using dew-point convergence. Preprints, *Ninth Conf. on Weather Forecasting and Analysis,* Seattle, WA, Amer. Meteor. Soc., 201–205.

Hudson, H. R., 1970: On the relationship between horizontal moisture convergence and convective cloud formation. ESSA Tech. Memo. ERLTM-NSSL 45, 29 pp.

_____, 1971: On the relationship between horizontal moisture convergence and convective cloud formation. *J. Appl. Meteor.*, **10**, 755–762.

Kain, J. S., M. E. Baldwin, and S. J. Weiss, 2003a: Parameterized updraft mass flux as a predictor of convective intensity. *Wea. Forecasting,* **18,** 106–116.

_____, M. E. Baldwin, P. R. Janish, S. J. Weiss, M. P. Kay, and G. W. Carbin, 2003b: Subjective verification Of numerical models as a component of a broader interaction between research and operations. *Wea. Forecasting,* **18**, 847-860.

Koch S. E., and J. McCarthy, 1982: The evolution of an Oklahoma dryline. Part II: Boundary-layer forcing of mesoconvective systems. *J. Atmos. Sci.,* **39,** 237–257.

Kuo, H. L., 1965: On formation and intensification of tropical cyclones through latent heat released by cumulus convection. *J. Atmos. Sci.*, **22**, 40–63.

_____, H. L., 1974: Further studies of the parameterization of the influence of cumulus convection on large-scale flow. *J. Atmos. Sci.*, **31**, 1232–1240.

Moller, A. R., 2001: Severe local storms forecasting. *Severe Convective Storms, Meteor. Monogr.* No. 50, Amer. Meteor. Soc., 433–480.

Moore, J. T., F. H. Glass, C. E. Graves, S. M. Rochette, and M. J. Singer, 2003: The environment of warm-season elevated thunderstorms associated with

heavy rainfall over the central United States. *Wea. Forecasting,* **18,** 861–878.

Negri, A. J., and T. H. Vonder Haar, 1980: Moisture convergence using satellite-derived wind fields: A severe local storm case study. *Mon. Wea. Rev.*, **108**, 1170–1182.

Newman, W. R., 1971: The relationship between horizontal moisture convergence and severe storm occurrences. M.S. thesis, School of Meteorology, University of Oklahoma, 54 pp. [Available from School of Meteorology, University of Oklahoma, 100 E. Boyd, Rm. 1310, Norman, OK 73019.]

Ostby, F. P., 1975: An application of severe storm forecast techniques to the outbreak of June 8, 1974. Preprints, *Ninth Conf. on Severe Local Storms,* Norman, OK, Amer.Meteor. Soc., 7–12.

Palmén, E., and E. O. Holopainen, 1962: Divergence, vertical velocity and conversion between potential and kinetic energy in an extratropical disturbance. *Geophysica*, **8**, 89–113.

Petterssen, S., 1956: *Weather Analysis and Forecasting.* Vol. I. 2d ed. McGraw-Hill, 428 pp.

Rasmusson, E. M., 1967: Atmospheric water vapor transport and the water balance of North America: Part I. Characteristics of the water vapor flux field. *Mon. Wea. Rev.,* **95,** 403–426.

Spar, J., 1953: A suggested technique for quantitative precipitation forecasting. *Mon. Wea. Rev.*, **81**, 217–221.

Ulanski, S. L., and M. Garstang, 1978: The role of surface divergence and vorticity in the life cycle of convective rainfall. Part I: Observations and analysis. *J. Atmos. Sci.*, **35**, 1047–1062.

Väisänen, A., 1961: Investigation of the vertical air movement and related phenomena in selected synoptic situations. *Commentationes Physico-Mathematicae, Societas Scientiarum Fennica,* **26**(7), 1–73.

Waldstreicher, J. S., 1989: A guide to utilizing moisture flux convergence as a predictor of convection. *Nat. Wea. Dig.*, **14**(4), 20–35.

Weckwerth, T., and coauthors, 2004: An overview of the International H_20 Project (IHOP_2002) and some preliminary highlights. *Bull. Amer. Meteor. Soc.*, **85**, 253-277.

Ziegler, C. L., and E. N. Rasmussen, 1998: The initiation of moist convection at the dryline: Forecasting issues from a case study perspective. *Wea. Forecasting*, **13**, 1106–1131.